

Article

# The Role of Highly-Resolved Gust Speed in Simulations of Storm Damage in Forests at the Landscape Scale: A Case Study from Southwest Germany

Christopher Jung <sup>1,\*</sup>, Dirk Schindler <sup>1</sup>, Axel Tim Albrecht <sup>2</sup> and Alexander Buchholz <sup>1</sup>

Received: 5 November 2015; Accepted: 25 December 2015; Published: 4 January 2016

Academic Editors: Robinson I. Negron-Juarez and Robert W. Talbot

<sup>1</sup> Environmental Meteorology, Albert-Ludwigs-University of Freiburg, Werthmannstrasse 10, Freiburg D-79085, Germany; dirk.schindler@meteo.uni-freiburg.de (D.S.); alex.buchholz@ymail.com (A.B.)

<sup>2</sup> Department of Forest Growth, Forest Research Institute Baden-Wuerttemberg, Wonnhaldestrasse 4, Freiburg D-79100, Germany; axel.albrecht@forst.bwl.de

\* Correspondence: christopher.jung@mail.unr.uni-freiburg.de; Tel.: +49-761-203-6822; Fax: +49-761-203-3586

**Abstract:** Routinely collected booking records of salvaged timber from the period 1979–2008 were used to empirically model the (1) storm damage probability; (2) proportions of storm-damaged timber and (3) endemic storm damage risk in the forest area of the German federal state of Baden-Wuerttemberg by applying random forests. Results from cross-validated predictor importance evaluation demonstrate that the relative impact of modeled gust speed fields on the predictive accuracy of the random forests models was greatest compared to the impact of forest and soil features. Forest areas prone to storm damage occurring within a period of five years were mainly located in mountainous upland regions where maximum gust speed exceeds 31 m/s in a five-year return period and conifers dominate the tree species composition. While mean storm damage probability continuously increased with increasing statistical gust speed proportions of storm-damaged timber peaked at a statistical maximum gust speed value of 29 m/s occurring in a five-year return period. Combining the statistical gust speed field with daily gust speed fields of two exceptional winter storms improved model accuracy and considerably increased the explained variance. Endemic storm damage risk was calculated from endemic storm damage probability and proportions of endemically storm-damaged timber. In combination with knowledge of local experts the storm damage risk modeled in a 50 m × 50 m resolution raster dataset can easily be used to identify areas prone to storm damage and to adapt silvicultural management regimes to make forests more windfirm.

**Keywords:** forest storm damage; high resolution gust speed field; statistical modeling; random forests; storms wiebke and lothar

## 1. Introduction

Storms influence forest ecosystems at multiple levels. They are key factors for forest composition, structure, demography, growth and ecosystem processes [1–3]. In European forests, storms caused 18.5 million m<sup>3</sup> of damaged timber per year over the period 1950–2000 [4]. At least 65% of all forest storm damage is caused by winter storms associated with the passage of high-impact low pressure fronts over Europe during the months November to January [5].

Exceptional winter storms that impacted Central Europe during the past decades were “Wiebke” in March 1990 [6], “Lothar” in December 1999 [7] and “Kyrill” in January 2007 [8]. With respect to the amount of damaged timber, storm Lothar, which passed Southwest Germany [9] and Switzerland [10] on 26 December 1999, was the most damaging event in these areas. In the aftermath of Lothar,

approximately 30 million m<sup>3</sup> of storm-damaged timber had to be salvaged in the German southwestern federal state Baden-Wuerttemberg corresponding to a monetary loss estimated at 770 million € [9,11].

Beside infrequent, catastrophic storms like Wiebke and Lothar, frequent, less intense storm events cause substantial amounts of endemically damaged timber [12] and chronically affect forest ecosystem services [13,14]. Endemic damage is damage due to regularly occurring storm events that are part of the local wind climate. An essential prerequisite for analysis and modeling of endemic forest storm damage is thus knowledge about statistical properties of the local wind climate which can be used to establish functional relationships between statistical wind fields and storm damage occurrence.

A variety of factors have an influence on forest storm damage formation. They can basically be differentiated into: weather conditions, orography, human influence, soil conditions and stand conditions [15]. Initially, high impact wind conditions may lead to damage and it is believed that in particular wind loads associated with strong gusts cause tree failure [16].

However, the predictive power of modeled storm-related gust speed fields was low in previous empirical storm damage modeling studies [12,17–20]. One reason for the low predictive power certainly was the coarse (often 1 km × 1 km) spatial resolution [12,17,19] which did not realistically represent the small scale nature of gusts. Furthermore, modeled gust speed fields were based on smoothed orography, which did not represent orographically complex terrain in sufficient detail. The combination of coarsely resolved gust speed and orography often resulted in a weak association between gust speed and terrain-related variables like topographic exposure [19,21] and elevation [20,22]. In fact, due to the better availability of datasets with a higher spatial resolution of topographic exposure and/or elevation, previous empirical forest storm damage models were often based on terrain-related proxy variables and not on high impact wind conditions [19,21].

The development of empirical forest storm damage models is generally based on a similar conceptual approach [19]: (1) mapping of storm-damaged areas; (2) mapping of environmental factors that might be directly or indirectly associated with forest storm damage; (3) estimation of the relative contribution of these factors to storm damage occurrence and/or storm damage amount and (4) calculation and classification of storm damage into different probability levels. Yet, in most previous studies damage probability calculations were based on only one or two exceptional storm events that led to catastrophic damage [17,19,20,23,24]. This means that in these studies results from damage probability modeling were presented and discussed based on the assumption that future storm events will occur under environmental conditions similar to those found for the few investigated exceptional cases, even though it is clear that storm damage events will rarely occur under similar environmental conditions again.

The goals of this study are therefore (1) separating the impact of catastrophic, infrequent storm events in forests from the impact of endemic storm events in the period 1979–2008 in the southwestern German federal state of Baden-Wuerttemberg; (2) quantifying the contribution of environmental factors to forest storm damage probability, proportions of storm-damaged timber for both catastrophic and endemic events as well as endemic storm damage risk and (3) building statistical models that are capable of predicting the five-year storm damage probability, proportions of storm-damaged timber in various periods and endemic storm damage risk on a high spatial resolution (50 m × 50 m).

All symbols, abbreviations and acronyms used in the text, are summarized in Table A1.

## 2. Material and Methods

### 2.1. Study Area

Storm damage probability, proportions of storm-damaged timber and storm damage risk were simulated in the forests of Baden-Wuerttemberg (Figure 1). Approximately 38% (13,700 km<sup>2</sup>) of the area of Baden-Wuerttemberg are covered with forests. The share of state-owned forests is 24%. The commercial forests in the study area are managed according to the guidelines of the state forest administration. According to Corine Land Cover data from the year 2000, close to half (45%) of the

forest area was covered by conifer-dominated forests. Mixed forests covered 35% and broad-leaved forests covered 20% [25]. The proportions of the forest types are very similar between state forests and non-state forests. A map showing the distribution of forest types in the study area can be found in [17]. The largest contiguous forest area is found in the low mountain range Black Forest with the highest elevations Feldberg (1496 m) in the south and Hornisgrinde (1164 m) in the north. A further prominent low mountain range is the Swabian Alb (highest elevations < 1020 m). To the west, the study area is bounded by the broad, flat Rhine Valley. A detailed summary of roughness and orographic features of the study area is given in [26].

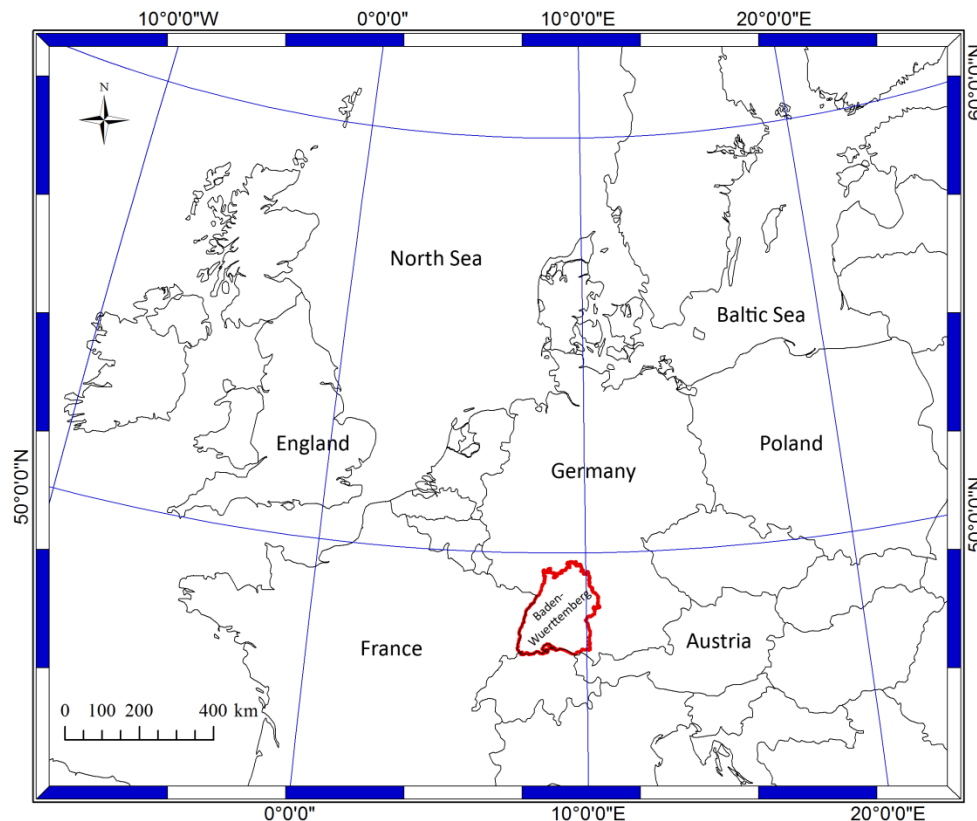


**Figure 1.** Extent of the study area Baden-Wuerttemberg in the southwest of Germany (red polygon).

## 2.2. Forest Damage Data

Annual booking records of salvaged timber were used to reconstruct the spatial storm damage pattern that occurred in the state forests during 1979–2008 ( $P_{30yr}$ ). The booking records contained information on the amount of storm-damaged timber and the total amount of harvested timber attributed to 15,871 forest compartments (average size ~20 ha). For the six five-year periods 1979–1983 ( $P_1$ ), 1984–1988 ( $P_2$ ), ..., 2004–2008 ( $P_6$ ), proportions of storm-damaged timber ( $DAM_{emp,i}$ ,  $i = 1, \dots, 6$ ) were calculated by dividing the cumulative amount of storm-damaged timber by the amount of all harvested timber for each compartment. Proportions of storm-damaged timber were compiled and analyzed for  $P_1$ – $P_6$  in order to account for the impact of “Wiebke” and “Lothar” and the subsequent delayed salvage-logging after the two storm events.

The choice of the period length was a trade-off between statistical representativity and the number of periods required to predict storm damage probability. Figure 2 shows the proportions of storm-damaged timber for  $P_{30yr}$  ( $DAM_{emp,30yr}$ ).

As can be seen in Figure 3,  $DAM_{emp,i}$  considerably differs between  $P_1$  to  $P_6$ . The high values of  $DAM_{emp,3}$  and  $DAM_{emp,5}$  result from the impact of the catastrophic storm events Wiebke and Lothar on the forests in Baden-Wuerttemberg. Storm Kyrill, which occurred in  $P_6$  caused

no discernable proportions of storm-damaged timber in the study area. The proportions of endemically storm-damaged timber ( $DAM_{emp,endemic}$ ) were calculated by averaging  $DAM_{emp,1}$ ,  $DAM_{emp,2}$ ,  $DAM_{emp,4}$  and  $DAM_{emp,6}$ .

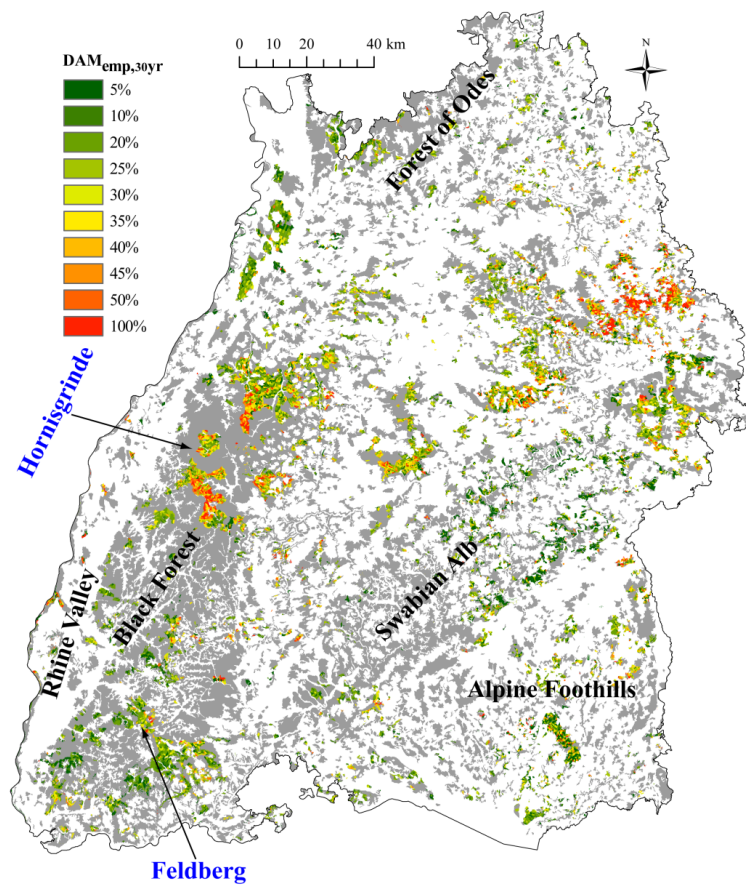


**Figure 2.** Map of proportions of storm-damaged timber in the period 1979–2008 ( $DAM_{emp,30yr}$ ). The legend values are highest class values. Grey areas indicate non-state forest areas for which no booking records are available. Blue arrow captions denote high mountain tops in the Black Forest.

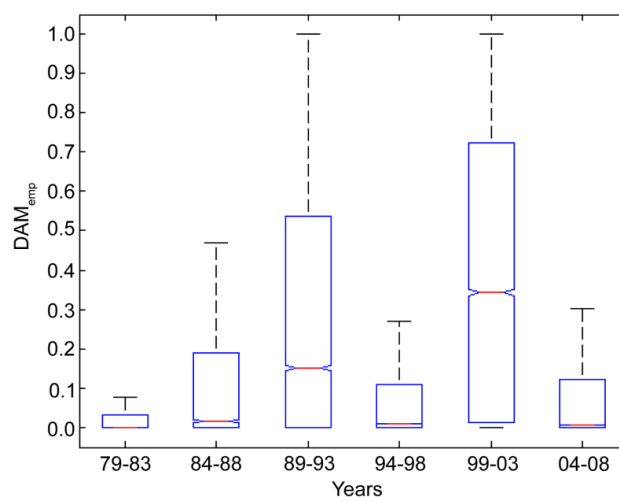


**Figure 3.** Boxplots of proportions of storm-damaged timber ( $DAM_{emp}$ ) in six five-year periods. Boxplot style: red lines indicate medians; boxes indicate interquartile ranges; whiskers indicate 1.5-times interquartile ranges.

$DAM_{emp,j}$ ,  $DAM_{emp,endemic}$  and  $DAM_{emp,30yr}$  were interpolated to 50 m  $\times$  50 m resolution raster datasets. The number of storm damage occurrences during  $P_1$ – $P_6$  is the raster cell-specific empirical classified storm damage probability ( $PC_{emp,j}$ ,  $j = 1, \dots, 7$ ) with  $PC_{emp,1}$  indicating that storm damage did not occur during the entire investigation period;  $PC_{emp,7}$  indicates that storm damage occurred in all six five-year periods. All datasets were prepared with the ArcGIS® 10.2 software (ESRI, Redlands, CA, USA).

### 2.3. Predictor Variables

Predictor variables that were available for random forests (RF) model building are listed in Table 1. Forest type (*FOR*) which consists of the three classes “conifer forest”, “broad-leaved” and “mixed forest”, was built from Corine Land Cover data. All soil related predictor variables were obtained from the Water and Soil Atlas of Baden-Wuerttemberg. Slope (*SL*) was calculated and classified from a digital terrain model.

The variable  $GS_{stat}$ , which represents the statistical properties of the near-surface gust speed field from the period 1979–2013 in the study area in either December ( $GS_{stat,Dec}$ ) or January ( $GS_{stat,Jan}$ ), is available from the study of [27]. It is a function of elevation, topographic exposure, roughness, aspect and reanalyzed wind speed at the 850 hPa pressure level. The  $GS_{stat}$ -values used in this study, were calculated for a return period of five years. All variables that were included in the gust speed modeling process were excluded from storm damage model building.

**Table 1.** List of predictor variables [19].

Predictor	Acronym	Scale	Classes	Data Source
Forest type	<i>FOR</i>	Categorical	3	LUBW <sup>1</sup>
Soil type	<i>SOIL</i>	Categorical	20	WSA <sup>2</sup>
Soil depth	<i>DEPTH</i>	Categorical	5	WSA <sup>2</sup>
Soil substrate	<i>SUB</i>	Categorical	17	WSA <sup>2</sup>
Soil acidification	<i>ACID</i>	Categorical	13	WSA <sup>2</sup>
Soil moisture regime	<i>MOIST</i>	Categorical	21	WSA <sup>2</sup>
Groundwater affected soils	<i>GRD</i>	Categorical	4	WSA <sup>2</sup>
Geology	<i>GEOL</i>	Categorical	14	WSA <sup>2</sup>
Slope	<i>SL</i>	Ordinal	7	LUBW <sup>1</sup>
Gust speed of December	$GS_{stat,Dec}$	Continuous	-	[27]
Gust speed of January	$GS_{stat,Jan}$	Continuous	-	[27]
Gust speed of 1 March 1990	$GS_{Wiebke}$	Continuous	-	According to [27]
Gust speed of 26 December 1999	$GS_{Lothar}$	Continuous	-	According to [27]

<sup>1</sup> LUBW: State Institute for Environmental Protection Baden-Wuerttemberg; <sup>2</sup> WSA: Water and Soil Atlas of Baden-Wuerttemberg.

The screening of the results from correlation analysis indicate that  $GS_{stat,Dec}$  and  $GS_{stat,Jan}$  were most strongly associated with storm damage. This is plausible since the highest gust speed values for a return period of five years occur in December and January in the study area [27]. Therefore, these gust speed fields were used for storm damage modeling. Focusing on  $GS_{stat,Dec}$  and  $GS_{stat,Jan}$  is in accordance with [5], who identified December and January as the months in which by far the highest amounts of storm-damaged timber occur in European forests. In Figure 4,  $GS_{stat,Dec}$  is mapped over the forest area. The strong variations of  $GS_{stat,Dec}$  on a small spatial scale, especially in the Black Forest, are due to the complex orography in the study area. The spatial resolution of all predictor variables is 50 m  $\times$  50 m. Further descriptions of the predictor variables are given in [19] and [27].

Multicollinearity among the predictor variables was investigated following [17] by assessing the variance inflation and the condition index in combination with variance-decomposition proportions according to [28]. However, no collinearity was detected among the predictor variables.

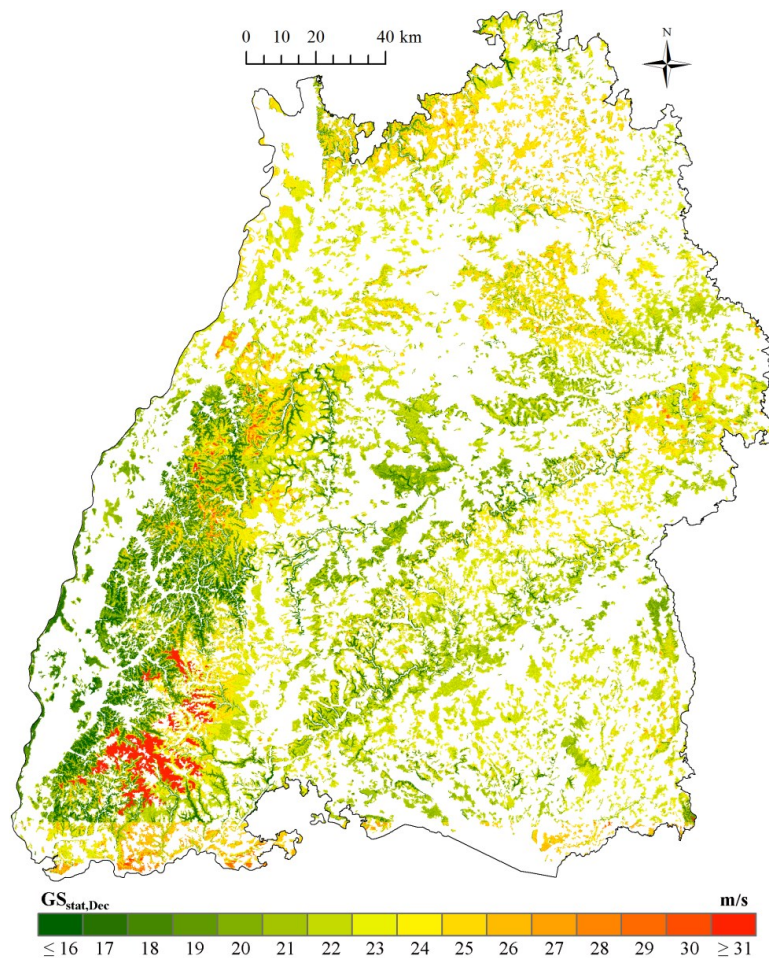


**Figure 4.** Map of statistical gust speed of December for a return period of five years ( $GS_{stat,Dec}$ ) covering the forest area.

#### 2.4. Model Building

To predict empirical storm damage probability ( $PC_{mod,j}$ ) and empirical proportions of storm-damaged timber ( $DAM_{mod}$ ) in the entire study area, the ensemble learning method random forests implemented in the Matlab<sup>®</sup> Statistics and Machine Learning Toolbox (The Math Works Inc., Natick, MA, USA, Release 2015a) was applied. The principle of RF is to combine many binary decision trees using bootstrap samples each containing 66% of the learning sample and randomly choosing a subset of predictors at each tree node [29]. The remaining 34% data left out are the out-of-bag (OOB) samples, which are used for cross-validation [30,31].

The RF-methodology was applied to simulate storm damage probability and proportions of storm-damaged timber because it can handle (1) nonlinear relationships [32]; (2) high-order interactions between predictor variables [32]; (3) noisy data [33,34]; (4) irrelevant predictor variables [35] and (5) a broad range of differently scaled data, including numeric and categorical data [32].

Bagged classification trees were used to model  $PC_{emp,j}$ . Bagged regression trees were used to model  $DAM_{emp,i}$ ,  $DAM_{emp,endemic}$  and  $DAM_{emp,30yr}$ . To quantify the impact of Wiebke and Lothar on the RF-modeling results (denoted by \*),  $GS_{Wiebke}$  and  $GS_{Lothar}$  were included in the model building process yielding  $DAM_{mod,3*}$ ,  $DAM_{mod,5*}$  and  $DAM_{mod,30yr*}$ . A summary of the RF-model outputs for P<sub>1</sub>–P<sub>6</sub> and the corresponding gust speed fields used for RF-model building is shown in Table 2. The RF-models were applied to simulate storm damage probability and proportions of storm-damaged timber for the entire forest area. From the modeled data, maps of classified storm damage probability and proportions of storm-damaged timber were produced.

The predictive accuracy of bagged classification trees was evaluated with a receiver operating characteristic (ROC) curve, which is a common measure for quantifying the accuracy of predictions [36,37]. For a model with high predictive power, ROC-curves steeply increase and the area under the curve (AUC) approaches a value of 1.0 whereas an AUC-value of 0.5 indicates limited predictive power. Predictive accuracy of regression trees was measured by mean squared error (MSE) and the coefficient of determination ( $R^2$ ).

**Table 2.** Summary of random forests (RF) model outputs for different periods (1–6, 30 year) and gust speed fields used to build the RF-models.

RF-Model Output	Periods							Gust Speed Field			
	1	2	3	4	5	6	30 Year	Wiebke	Lothar	Stat,December	Stat,January
$DAM_{mod,30yr}$							●			●	
$DAM_{mod,1}$	●									●	
$DAM_{mod,2}$		●								●	
$DAM_{mod,3}$			●								●
$DAM_{mod,4}$				●						●	
$DAM_{mod,5}$					●					●	
$DAM_{mod,6}$						●					●
$DAM_{mod,endemic}$	●	●		●		●				●	
$DAM_{mod,30yr*}$							●	●	●	●	
$DAM_{mod,3*}$			●					●			●
$DAM_{mod,5*}$					●				●		

### 2.5. Predictor Importance

The contribution of individual predictor variables to final RF-model outputs was evaluated by the predictor importance (PI) which was measured for OOB. The basic idea behind PI is to identify predictor variables which affect RF-model accuracy only little after being randomly permuted. In contrast, important predictor variables strongly change model accuracy after being randomly permuted. Model accuracy is measured before and after permuting a predictor variable for each tree [29,38–40]. The PI-values thus represent for (1) RF-classification models the relative misclassification increase as compared to the OOB-misclassification; (2) RF-regression models the relative increase in MSE as compared to the OOB-MSE [38]. The decision whether to integrate  $GS_{stat,Dec}$  or  $GS_{stat,Jan}$  in the final RF-models was based on PI.

### 2.6. Risk Modeling

The endemic storm damage risk related to a five-year period without exceptional storm events ( $RC_{emp,endemic}$ ) was calculated according to

$$RC_{emp,endemic} = DAM_{emp,endemic} \cdot PC_{emp,endemic} \tag{1}$$

with  $PC_{emp,endemic}$  being calculated and classified based on storm damage occurrence in  $P_1, P_2, P_4$  and  $P_6$ . Based on the  $RC_{emp,endemic}$ -values a risk matrix (Figure 5) was produced according to [41]. The  $DAM_{emp,endemic}$ -values were assigned to five classes (0%–6%, 7%–14%, 15%–24%, 25%–37%, 38%–55%) using natural breaks yielding severity (negligible, minor, moderate, extensive, serious). Storm damage risk was divided into the four risk indexes low, moderate, high and very high. To provide easily accessible information on  $RC_{emp,endemic}$ , it was modeled in the entire study area using a RF-model ( $RC_{mod,endemic}$ ). The importance of the predictor variables (risk factors) for  $RC_{mod,endemic}$  was evaluated by PI.

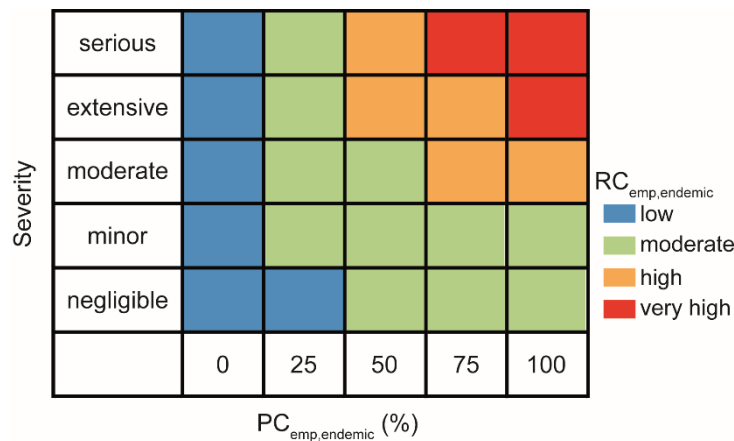


**Figure 5.** Combinations of severity and empirical probability of endemic storm damage events ( $PC_{emp,endemic}$ ) used to classify empirical endemic storm damage risk ( $RC_{emp,endemic}$ ).

### 3. Results and Discussion

#### 3.1. Predictor Importance

##### 3.1.1. Damage Probability

Results from *PI*-evaluation associated with the calculation of  $PC_{mod,j}$  demonstrate that the relative impact of  $GS_{stat,Dec}$  on the predictive accuracy of the RF-model was greatest ( $PI = 19.1$ ). A predictor variable nearly equally important for RF-model accuracy as  $GS_{stat,Dec}$  was *FOR* ( $PI = 18.3$ ) which is in good agreement with findings reported for the study area in previous investigations [17,19]. Also important for the RF-modeling performance was *MOIST* ( $PI = 11.9$ ). The soil moisture regime is known to have great influence on windfirmness of trees. In moist soils, root development is often hampered [42,43] and root anchorage is lower as compared with drier soils [44,45]. In this study, all other predictor variables that have been shown to be of importance for storm damage occurrence like soil type [17,19] or soil acidification [46] are of minor importance ( $PI < 10$ ) for classification of storm damage probability.

According to our knowledge, this is the first time that gust speed was found to be the most important predictor variable to be used in empirical storm damage modeling. In our opinion, this is mainly because the spatial resolution of the available gust speed fields (50 m × 50 m) is far more detailed than the gust speed data available in previous studies [12,17–19]. The high-resolution gust speed models incorporate roughness and topographic features, which had to be neglected or considered separately in earlier investigations.

It is clear that the proposed modeling approach does not include all variables that are involved in forest storm damage occurrence. Based on findings from previous studies, it is plausible that variables like tree height [24,47,48], tree species [20,48] or forest management [18,48] are important predictor variables for damage occurrence as well. However, these variables were not available at the landscape scale.

Further indication for the plausibility and importance of  $GS_{stat}$ -fields for  $PC_{mod,j}$  is the dependence of the proportions of forest area associated with  $PC_{emp,j}$  on  $GS_{stat,Dec}$ . Results shown in Figure 6a demonstrate that the proportion of forest area associated with  $PC_{emp,1}$ , which represents the forest area without damage (binary result: storm damage no) over the entire investigation period, is substantially higher for  $GS_{stat,Dec} \leq 16$  m/s (6.8%) than for  $GS_{stat,Dec} \geq 31$  m/s (1.4%). This means that with increasing  $GS_{stat,Dec}$  the proportion of undamaged forest area decreases. On the other hand, the proportion of forest area associated with  $PC_{emp,7}$  which represents damage occurrence in all six five-year periods, increases with increasing gust speed from 9.9% for  $GS_{stat,Dec} \leq 16$  m/s to 35.8% for  $GS_{stat,Dec} \geq 31$  m/s (Figure 6b).



The results from the *PI*-evaluation for  $DAM_{mod,30yr*}$  demonstrate that  $GS_{stat,Dec}$ ,  $GS_{Wiebke}$  and  $GS_{Lothar}$  are the most important predictor variables (Figure 7). In agreement with the empirical proportions for storm-damaged timber that were presented in Figure 3, the *PI*-value for  $GS_{Lothar}$  is higher than for  $GS_{Wiebke}$ .

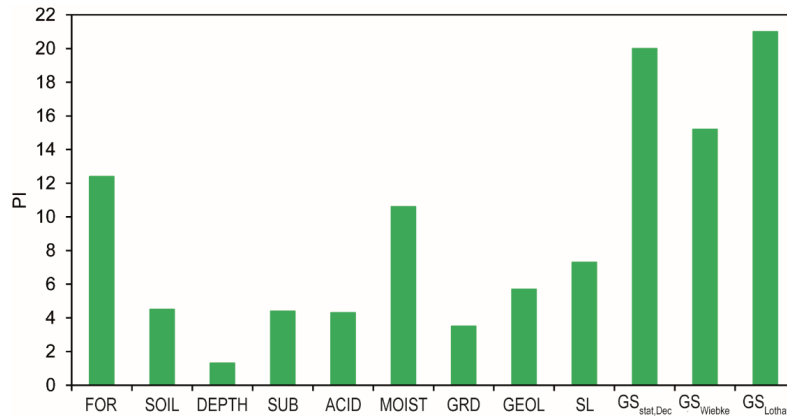


**Figure 7.** Predictor Importance (*PI*) of random forests model output for modeled proportions of storm-damaged timber in the period 1979–2008 with Wiebke and Lothar gust speed fields being included in model building.

### 3.1.3. Damage Risk

The importance of the risk factors for RF-model output  $RC_{mod,endemic}$  is similar to the importance of predictor variables for  $PC_{mod,j}$  and  $DAM_{mod,endemic}$  (Figure 8). The most important risk factor was  $GS_{stat,Dec}$  ( $PI = 19.0$ ) followed by  $MOIST$  ( $PI = 15.7$ ) and  $FOR$  ( $PI = 12.5$ ). All other risk factors were only of minor importance for  $RC_{mod,endemic}$  ( $PI < 10$ ).

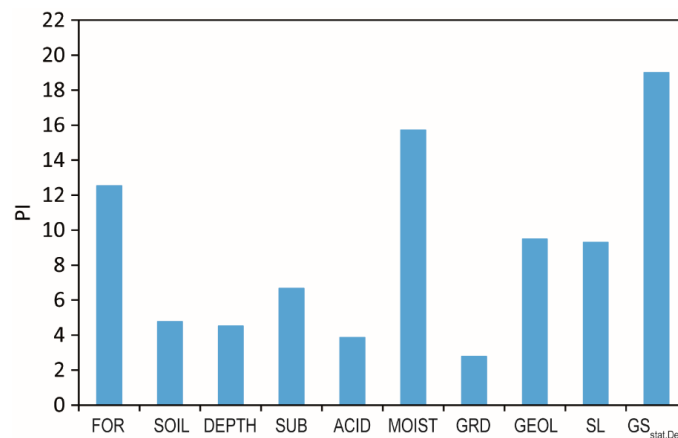


**Figure 8.** Predictor Importance (*PI*) of random forests model output for modeled endemic storm damage risk.

### 3.2. Mapping of Damage Probability

Results from ROC-curve evaluation of the OOB-samples of  $PC_{mod,j}$  ( $PC_{OOB,j}$ ) show that the cross-validated *AUC*-value for  $PC_{OOB,1}$ , which represents the damage probability class “no damage”, is higher ( $AUC = 0.86$ ) than in previous studies [12,17,19,49] (Figure 9). The *AUC*-values that are associated with  $PC_{OOB,2}$ – $PC_{OOB,7}$  vary between 0.74 and 0.81.  $PC_{OOB,2}$ – $PC_{OOB,7}$  define more precisely the probability of damage occurrence in  $P_{30yr}$ . The more precise division of  $PC_{mod,j}$  was enabled by the inclusion of highly-resolved gust speed fields into the RF-model building process.

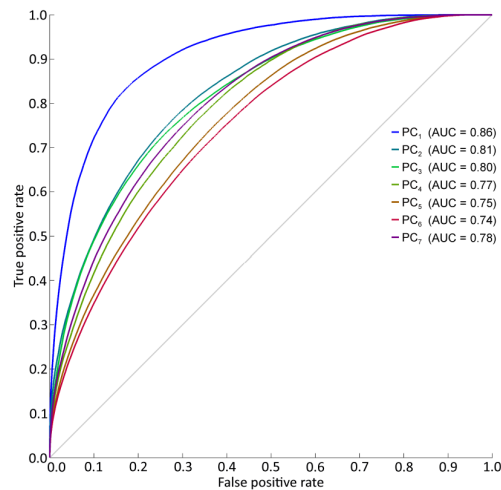


**Figure 9.** Receiver operating curves for modeled classified storm damage probability and the associated area under curve (AUC) values.

It is very likely that the accuracy of the obtained modeling results would improve when damage data, which are at the moment associated with forest compartments, become available as a raster dataset at a higher spatial resolution.

As an example for RF-model performance, Figure 10 compares  $PC_{emp}$  (Figure 10a,d) with  $PC_{mod}$  (Figure 10b,e) for two small parts of the state forest area. Results presented in Figure 10c,f illustrate the application of the RF-model to all types of forest ownership found in the presented map extracts.

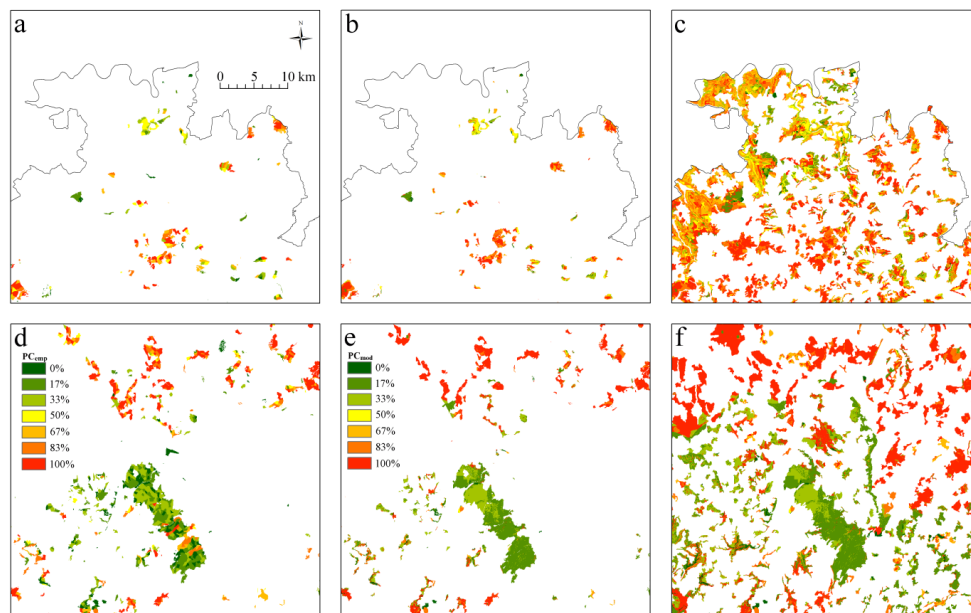


**Figure 10.** Two examples of (a,d)  $PC_{emp}$ ; (b,e)  $PC_{mod}$  for the state forest; (c,f)  $PC_{mod}$  for all types of forest ownership in the presented map extract.

The functional dependence of the averaged probability classes of the OOB-samples ( $PC_{OOB,mean}$ ) on  $GS_{stat,Dec}$  is quantified by a second order polynomial in Figure 11. The high value of the coefficient of determination ( $R^2 = 0.96$ ) indicates that the relationship between  $PC_{OOB,mean}$  and  $GS_{stat,Dec}$  is strong.  $PC_{OOB,mean}$  increases from 0.66 at  $GS_{stat,Dec} \leq 16$  m/s to 0.93 at  $GS_{stat,Dec} \geq 31$  m/s. The steeper increase of the polynomial at higher values of  $GS_{stat,Dec}$  might be the result of the basically quadratic relationship between near-surface wind field properties and wind loading on trees [50].

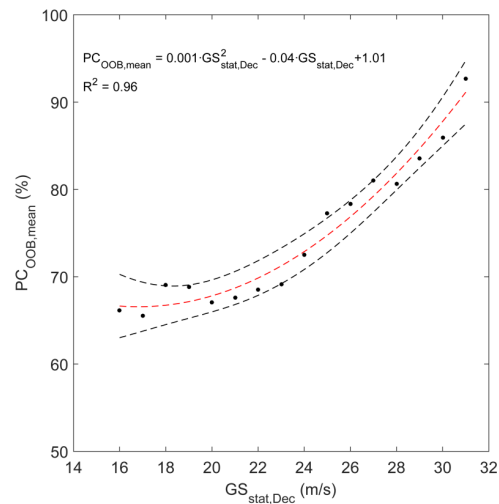


**Figure 11.** Out-of-bag samples of averaged probability class of modeled classified storm damage probability ( $PC_{OOB,mean}$ ) as a function of statistical gust speed of December for a return period of five years ( $GS_{stat,Dec}$ ).

The evaluation of  $PC_{mod,j}$  exhibits that 67% of all  $PC_{mod,j}$ -classes are assigned to  $PC_{mod,5}$ – $PC_{mod,7}$  ( $PC_{mod,1}$ : 8%;  $PC_{mod,2}$ : 8%;  $PC_{mod,3}$ : 12%;  $PC_{mod,4}$ : 5%;  $PC_{mod,5}$ : 12%;  $PC_{mod,6}$ : 28%;  $PC_{mod,7}$ : 27%). A map of  $PC_{mod}$  (Figure 12) illustrates that in large parts of the forest area  $PC_{mod}$ -values are higher than 50% which means that storm damage is likely for a return period of 5 years. Only large parts of the Swabian Alb and the Rhine Valley are less threatened by high-impact storm events. The lower storm damage probability in these two parts of the study area mainly results from low  $GS_{stat,Dec}$ -values, dry soils and the predominance of broad-leaved and mixed forests. Highest  $PC_{mod}$ -values occur in large parts of the Black Forest, in the northern part of the Alpine Foothills and in the northern parts of Baden-Wuerttemberg where  $GS_{stat,Dec}$  is high, soils are fresh or temporarily fresh and conifers predominate.

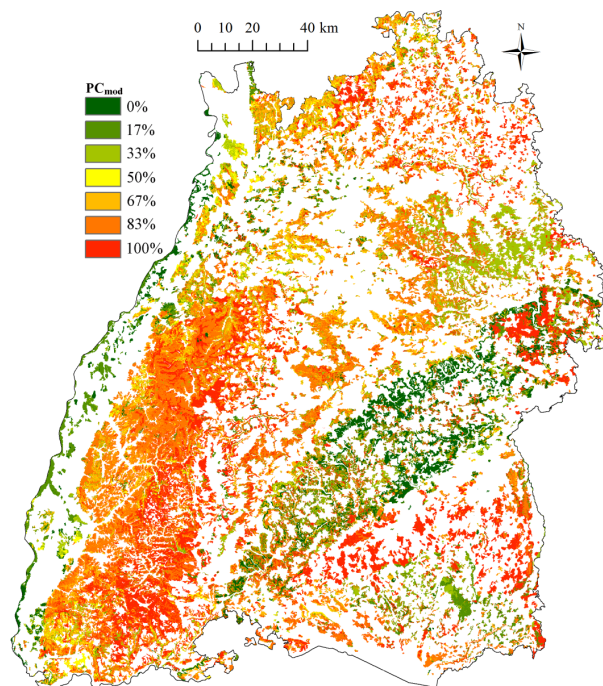


**Figure 12.** Map of modeled storm damage probability ( $PC_{mod}$ ).

### 3.3. Mapping of Damage Proportions

Results from OOB-evaluation of  $DAM_{mod}$ -model performance are presented in Table 4 ( $DAM_{OOB}$ ). The MSE-values for the RF-model outputs  $DAM_{OOB,30yr}$  and  $DAM_{OOB,endemic}$  are  $MSE = 0.02$  and  $MSE = 0.01$ . The explained variance as quantified by  $R^2$  equals to 0.30 and 0.28 which is better than analogous results from previous studies [12,18]. RF-Model accuracy clearly increased for  $DAM_{OOB,3}$  and  $DAM_{OOB,5}$  from  $MSE = \{0.08, 0.10\}$  and  $R^2 = \{0.25, 0.22\}$  to  $MSE = \{0.07, 0.07\}$  and  $R^2 = \{0.36, 0.41\}$  when  $GS_{Wiebke}$  ( $DAM_{OOB,3*}$ ) and  $GS_{Lothar}$  ( $DAM_{OOB,5*}$ ) are included into RF-model development. Highest model accuracy ( $R^2 = 0.53$  and  $MSE = 0.01$ ) was achieved when  $GS_{stat,Dec}$ ,  $GS_{Wiebke}$  and  $GS_{Lothar}$  are used in combination to model proportions of storm-damaged timber from 1979 to 2008 ( $DAM_{OOB,30yr*}$ ). The clear increase of  $R^2$  suggests that the gust speed fields related to Wiebke and Lothar substantially differ from the statistical gust speed field and thus explain an additional large part of variance in  $DAM_{emp,30yr}$ -data.

**Table 4.** Summary of out-of-bag-MSE and  $-R^2$  calculated from RF-model output.

		RF-Model Output						
	$DAM_{OOB,3}$	$DAM_{OOB,5}$	$DAM_{OOB,endemic}$	$DAM_{OOB,30yr}$	$DAM_{OOB,3*}$	$DAM_{OOB,5*}$	$DAM_{OOB,30yr*}$	
MSE	0.08	0.10	0.01	0.02	0.07	0.07	0.01	
$R^2$	0.25	0.22	0.28	0.30	0.36	0.41	0.53	

Figure 13a,b compare  $DAM_{emp,30yr}$  with  $DAM_{mod,30yr}$  for the region around the Hornisgrinde in the northern Black Forest. The region is characterized by a pronounced variability of  $GS_{stat,Dec}$ -values (Figure 13c,f). This variability is caused by orographically complex terrain and large variations in elevation across all forest types (Figure 13d). The transfer of  $DAM_{mod,30yr}$  to all types of forest ownership found in the Corine data-based map extract also gives plausible values (Figure 13e). It is therefore concluded that this example demonstrates (1) appropriate accuracy of  $DAM_{mod,30yr}$  in complex terrain; (2) the portability of  $DAM_{mod,30yr}$  to all types of forest ownership and (3) the dependency of  $DAM_{mod,30yr}$  on  $GS_{stat,Dec}$  and FOR.

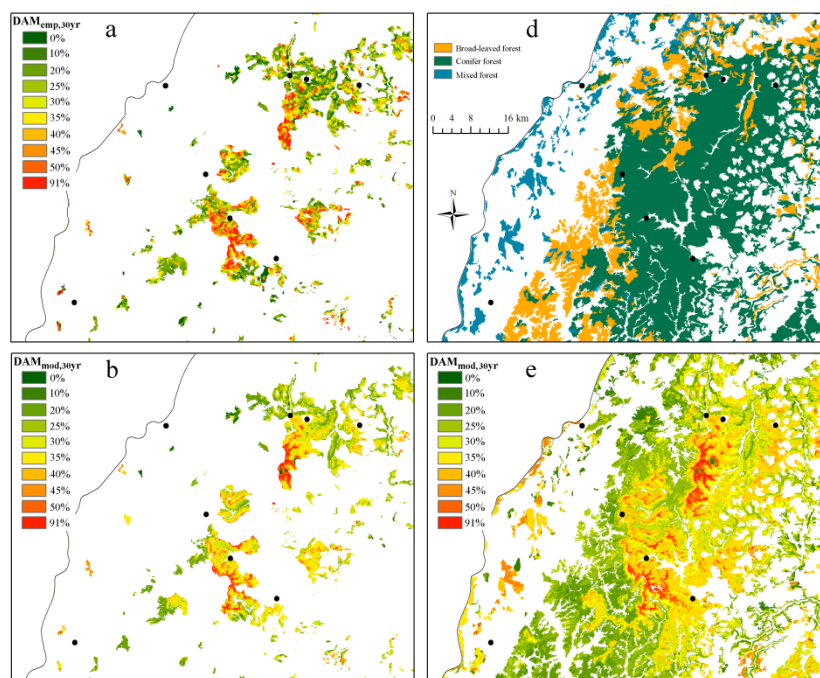


**Figure 13.** Cont.

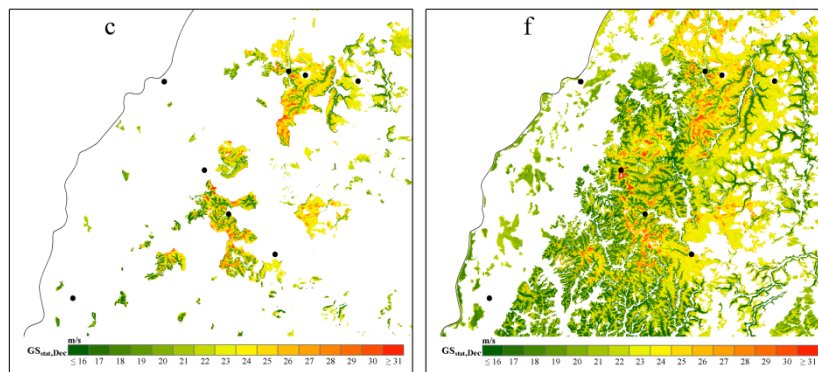


**Figure 13.** Map extract showing (a–c)  $DAM_{emp,30yr}$ ,  $DAM_{mod,30yr}$ ,  $GS_{stat,Dec}$  for state forests; (d–f)  $FOR$ ,  $DAM_{mod,30yr}$  and  $GS_{stat,Dec}$  over all types of forest ownership in the northern Black Forest. The black dots indicate the locations of meteorological stations in this area used to build the gust speed model. The legend values indicate highest class values.

The functional relationships between  $GS_{Wiebke}$ ,  $GS_{Lothar}$  and  $GS_{stat,Dec}$  and OOB-samples of modeled proportions of storm-damaged timber are shown in Figure 14a–c. From this it is clear that an increase of median  $DAM_{OOB}$  can be linked to an increase of gust speed. In the range of gust speed values measured during the passage of Wiebke, the medians of  $DAM_{OOB,3*}$  take values ranging from 0.16 at  $GS_{Wiebke} = 12$  m/s to 0.60 at  $GS_{Wiebke} = 51$  m/s. The  $DAM_{OOB,5*}$ -median values associated with Lothar increase from 0.32 ( $GS_{Lothar} = 15$  m/s) to 0.81 ( $GS_{Lothar} = 57$  m/s) with interquartile ranges of  $DAM_{OOB,5*}$  for  $GS_{Lothar} \geq 48$  m/s being considerably lower than for  $GS_{Lothar} < 48$  m/s. This finding leads to the conclusion that for very high  $GS_{Lothar}$ -values the proportions of storm-damaged timber is exceptionally high, regardless of other factors influencing proportions of storm-damaged timber. The differences in  $DAM_{OOB,3*}$  and  $DAM_{OOB,5*}$  between corresponding  $GS_{Wiebke}$ - and  $GS_{Lothar}$ -classes result from damage that was caused by the passage of storms other than Wiebke and Lothar in  $P_3$  and  $P_5$ .

Highest  $GS_{stat,Dec}$ -values are clearly lower than  $GS_{Wiebke}$ - and  $GS_{Lothar}$ -values. The corresponding  $DAM_{OOB,30yr}$ -median values nonetheless increase from 0.16 at  $GS_{stat,Dec} \leq 16$  m/s to 0.29 at  $GS_{stat,Dec} = 29$  m/s. However,  $DAM_{OOB,30yr}$ -median values are clearly lower than  $DAM_{OOB}$ -values dependent on  $GS_{Wiebke}$  and  $GS_{Lothar}$ .

The reasons for the decrease of  $DAM_{OOB,30yr}$ -median values at highest  $GS_{stat,Dec}$ -values are open to speculation. One reason might be that by far the largest proportion of highest  $GS_{stat,Dec}$ -values occurs at highest elevations in the southern Black Forest around the Feldberg. Therefore, decreasing proportions of storm-damaged timber at these elevations might be due to acclimative tree growth in response to recurrently high wind loading that increases tree stability against excessive wind exposure [20,51–54]. Another reason might be the limited predictive accuracy of the applied gust speed model at elevations higher than 1200 m a.s.l. due to finite availability of meteorological stations at which gust speed is measured [27]. Furthermore, in the applied gust speed model airflow is parameterized to be more laminar at highest elevations, like the Feldberg region, which reach the top of the atmospheric boundary layer.

The relationships between  $FOR$  and  $DAM_{OOB}$  are presented in Figure 14d–f. The variability of  $DAM_{OOB,3*}$ ,  $DAM_{OOB,5*}$  and  $DAM_{OOB,30yr}$  as a function of gust speed is greater than the variability of  $DAM_{OOB}$  as a function of  $FOR$  which is interpreted to mean that the variability of gust speed is more informative for the explanation of  $DAM_{OOB}$  than  $FOR$ . The median values of  $DAM_{OOB}$  are always lowest for mixed forests (between  $DAM_{OOB,30yr} = 0.15$  and  $DAM_{OOB,5*} = 0.24$ ) and highest for conifers (between  $DAM_{OOB,30yr} = 0.26$  and  $DAM_{OOB,5*} = 0.47$ ). This effect might be due to higher drag of evergreen conifers in winter when most high-impact storms occur in the study area [55] while broad-leaved tree species are leafless [46,56,57].

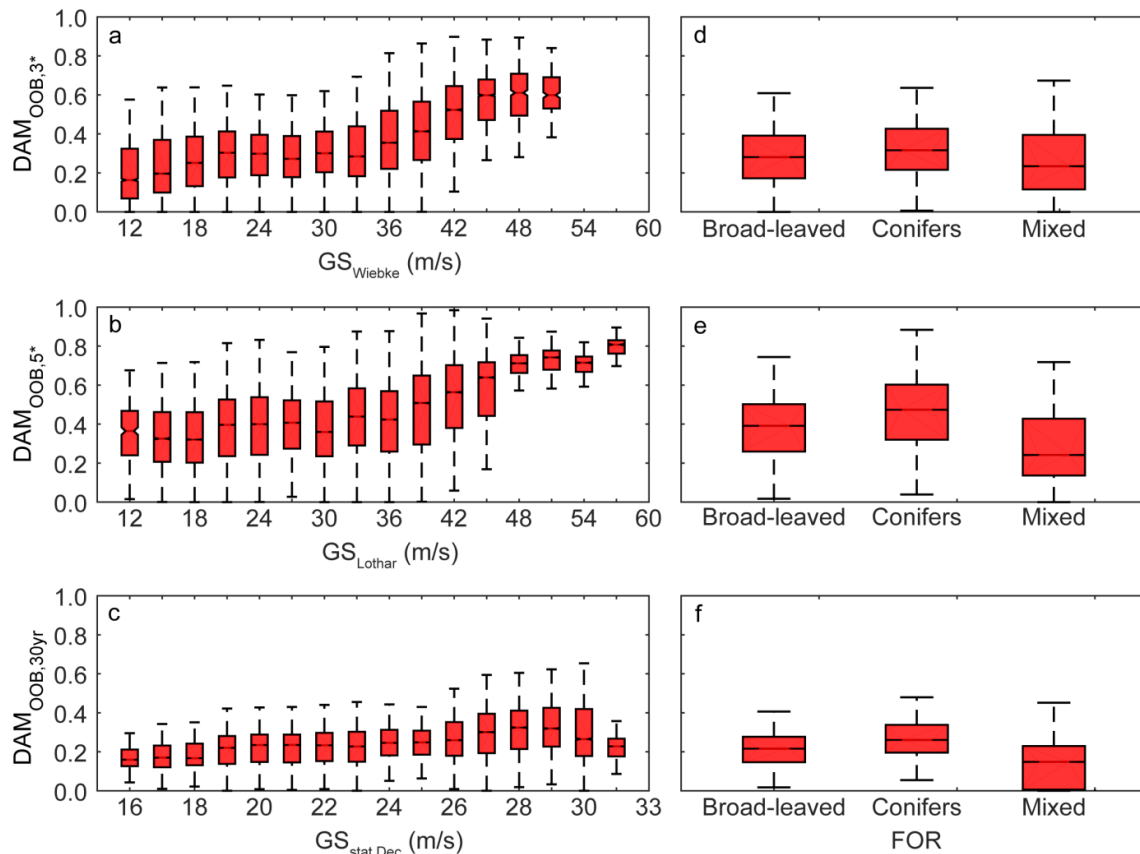


**Figure 14.** Boxplot of  $DAM_{OOB,3*}$  as a function of  $GS_{Wiebke}$  (a);  $DAM_{OOB,5*}$  as a function of  $GS_{Lothar}$  (b);  $DAM_{OOB,30yr}$  as a function of  $GS_{stat,Dec}$  (c);  $DAM_{OOB,3*}$  (d);  $DAM_{OOB,5*}$  (e) and  $DAM_{OOB,30yr}$  as a function of FOR (f).

A map of the modeled proportions of endemically storm-damaged timber (Figure 15) shows that the highest  $DAM_{mod,endemic}$ -values (up to 55%) occur mostly in the northern Black Forest in exposed areas at high elevations. Other areas prone to endemic storm damage are in the Forests of Odes and the northern Alpine Foothills. Apart from these regions,  $DAM_{mod,endemic}$ -values higher than 20% do not occur over wide areas (7%). Lowest  $DAM_{mod,endemic}$ -values ( $\leq 5\%$ ) can be found in 16% of the forest area. These areas, which are not prone to storm damage, are mainly located in the deep Rhine Valley and in narrow valleys of the Swabian Alb where statistical wind speed values are low [26].

Although it is clear that the proportions of endemically storm-damaged timber is rather small in the entire study area compared to the catastrophic proportions of storm-damaged timber, endemic storm events can regionally be an important disturbance factor. According to our calculations, endemic storm events can cause up to 55% of the total amount of salvaged timber. This is particularly the case when forest composition is dominated by conifers and  $GS_{stat,Dec}$ -values are in the range 25–30 m/s.

On the other hand, endemic storm damage is of minor importance when the forest composition is a mixture of conifers and broad-leaved tree species and  $GS_{stat,Dec}$ -values are below 20 m/s. Thus, it can be stated that these results provide a valuable basis for a first assessment of forest areas generally prone to endemic storm damage.

In order to localize and quantify the exceptional nature of storm Lothar in connection with forest storm damage, the difference between  $DAM_{mod,5*}$  and  $DAM_{mod,endemic}$  is mapped in Figure 16.

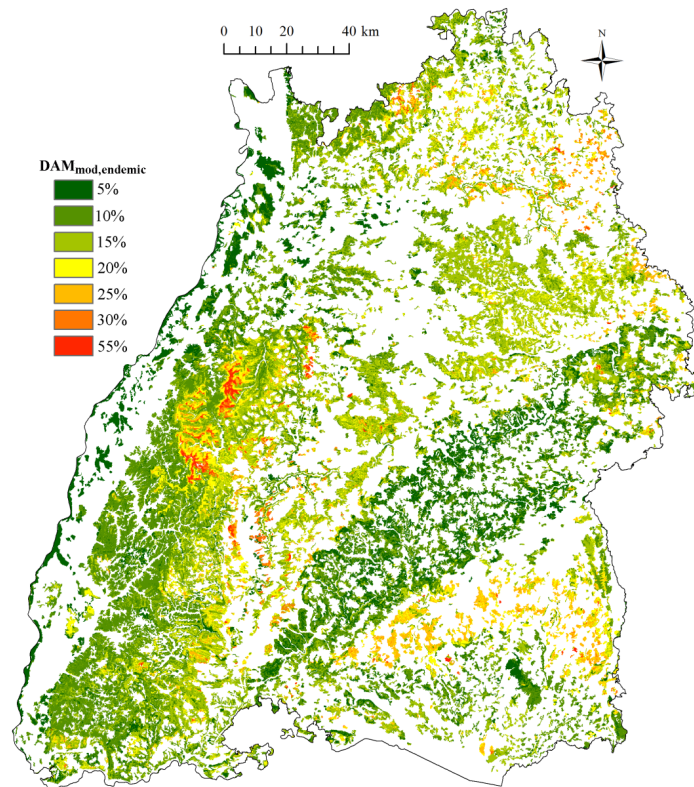


**Figure 15.** Map of modeled proportions of endemically storm-damaged timber ( $DAM_{mod,endemic}$ ). The legend values indicate highest class values.

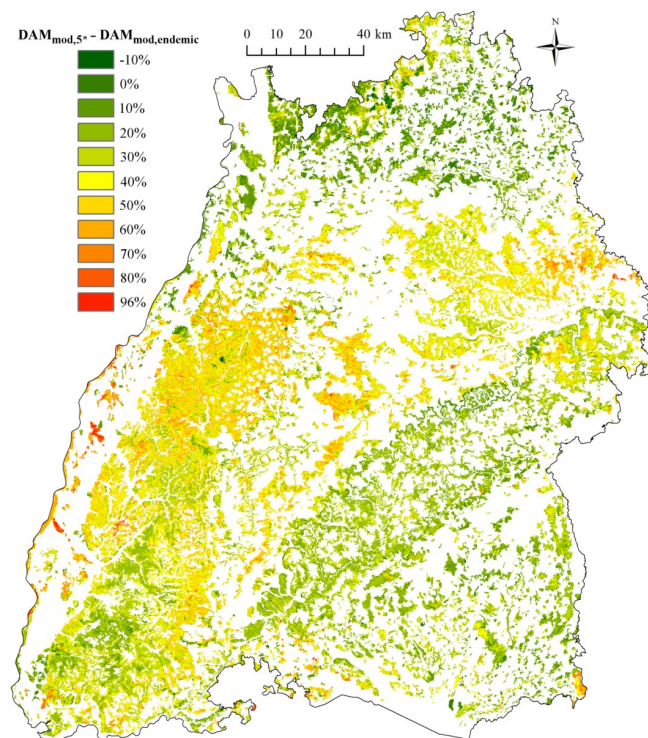


**Figure 16.** Difference map of modeled proportions of storm-damaged timber in the period 1999–2003 with Lothar gust speed field being included in model building ( $DAM_{mod,5*}$ ) and modeled proportions of endemically storm-damaged timber  $DAM_{mod,endemic}$ . The legend values indicate highest class values.

The difference between both models is remarkable. Especially, in parts of the deep Rhine Valley  $DAM_{mod,5*}$ -values are up to 96% higher than  $DAM_{mod,endemic}$ -values. This might be the result of low  $GS_{stat,Dec}$ -values which indicate low chronic wind loading on trees and thus limited acclimative tree growth. However, in this area,  $GS_{Lothar}$ -values often exceeded 35 m/s causing catastrophic proportions of storm-damaged timber. Other parts of the study area, where  $DAM_{mod,5*}$ -values were also considerably higher (40%–50%) after the passage of Lothar, are located in the northern Black Forest and Virngrund. Overall, in 10% of the forest area the difference between  $DAM_{mod,5*}$  and  $DAM_{mod,endemic}$  was higher than 50%.

In contrast to the severely damaged parts of the study area, the northern part remained virtually undamaged because  $GS_{Lothar} \leq 20$  m/s. In some parts of this region (4%),  $DAM_{mod,5*}$ -values were even below  $DAM_{mod,endemic}$ -values.

The proportions of storm-damaged timber in the period 1979–2008 are shown in Figure 17. As for  $DAM_{mod,endemic}$ , highest  $DAM_{mod,30yr*}$ -values occur in the northern Black Forest, in the Forests of Odes, Virngrund and parts of the Rhine Valley reaching up to 91%.

The mapped storm damage pattern results from the impacts of storms Wiebke and Lothar as well as the statistical gust speed field. While the northern part of the Black Forest is affected both by the statistical gust speed field and the exceptional gust speed fields associated with Wiebke and Lothar, Wiebke especially caused damage in the Forest of Odes, and Lothar devastated forests in the Rhine Valley and Virngrund. Over the entire investigation period, there was only minor damage to forests located in narrow valleys of the Swabian Alb.

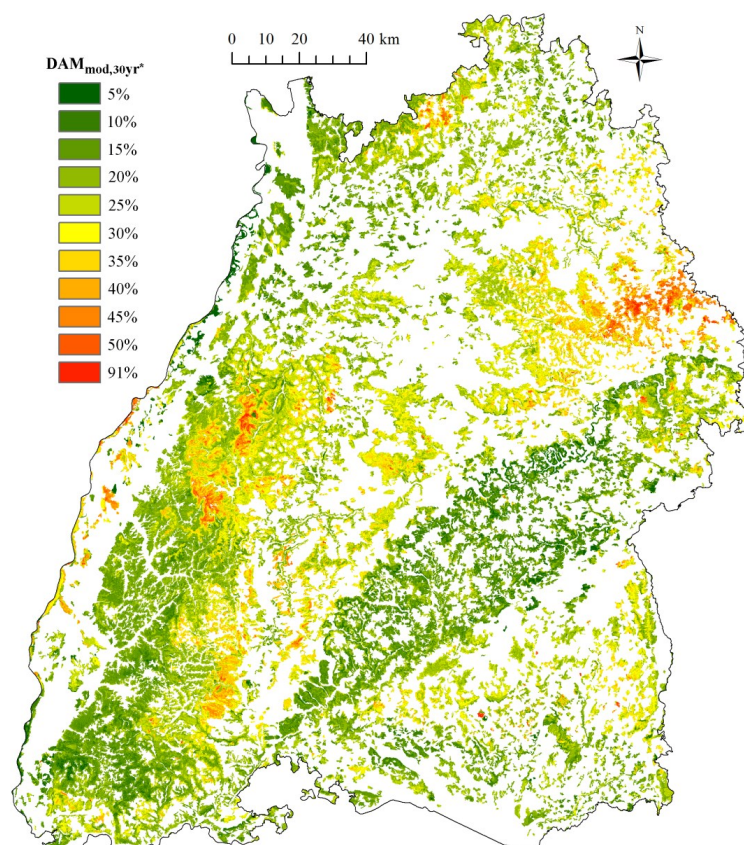


**Figure 17.** Map of modeled proportions of storm-damaged timber in the period 1979–2008 with Wiebke and Lothar gust speed fields being included in model building ( $DAM_{mod,30yr*}$ ). The legend values indicate highest class values.

### 3.4. Mapping of Damage Risk

ROC-curve based evaluation of the OOB-samples of  $RC_{mod,endemic}$  ( $RC_{OOB,endemic}$ ) exhibits that RF-model accuracy is best for low ( $AUC = 0.83$ ) and very high ( $AUC = 0.82$ ) storm damage risk. For moderate and high storm damage risk RF-model accuracy is slightly lower ( $AUC = 0.72$  and  $AUC = 0.76$ ). The observed risk-related  $AUC$ -value pattern corresponds to results that were presented in Figure 14. They indicate that at very low gust speed, storm damage risk is low, while at very high gust speed, storm damage risk is very high. In the moderate and high storm damage risk indexes, the influence of gust speed is superimposed by other environmental factors like forest type and soil moisture. Prominent, extended areas exposed to very high storm damage risk are located in parts of the northern Black Forest and the north-eastern part of Baden-Wuerttemberg (Figure 18). Forested areas at low storm damage risk are the Rhine Valley and the valleys of the Swabian Alb.

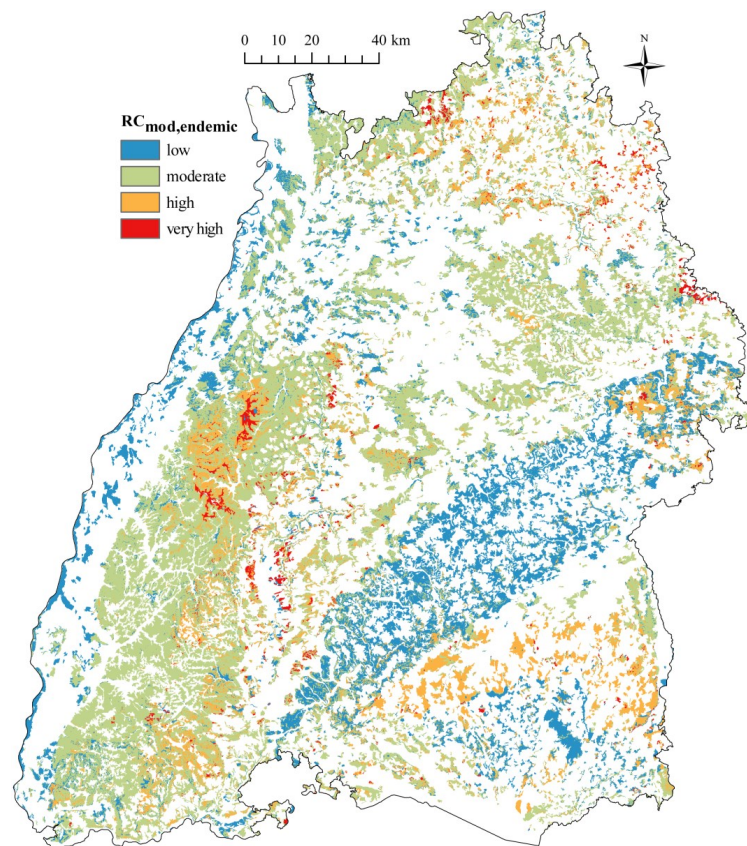


Figure 18. Map of modeled endemic storm damage risk ( $RC_{mod,endemic}$ ).

## 4. Conclusions

The presented statistical modeling approach allows for the analysis of storm damage probability and proportions of storm-damaged timber at the landscape scale at very high spatial resolution ( $50\text{ m} \times 50\text{ m}$ ). It is based on five-year aggregated booking records and enables the distinction between endemic and catastrophic storm damage proportions for the period 1979–2008. This means that the proposed methodology opens up the possibility to embed damage caused by exceptional storms like Wiebke and Lothar into the regional chronic damage pattern. In the context of empirical-statistical storm damage modeling this is an important achievement, because consideration of single storm events might bias the assessment of storm damage predictor importance since every storm event is unique concerning intensity, spatial extent and duration [23]. Including high-resolution statistical gust speed fields [27] into storm damage modeling process clearly improves model accuracy in comparison

to previous studies when only lower resolution gust speed fields were available [17,19]. The results obtained for the probability and proportions of endemically storm-damaged timber can be regarded as estimates of endemic storm damage risk.

Given that predictor variables similar to the predictor variables that have been used in this study are available, the methodology can easily be transferred to other areas. An important task for the future will be the inclusion of convective, localized storm events which mainly occur during summertime in the study area [58–60].

In combination with knowledge of local experts, the modeling approach can then be used to identify areas prone to storm damage and to initiate the adaption of silvicultural management regimes to make forests more windfirm in high and very high storm damage risk areas. Based on our findings an effective measure could be the conversion of coniferous forests to either broad-leaved or mixed forests.

**Author Contributions:** Christopher Jung developed the research idea, carried out data analysis, built and mapped the RF-models and wrote the manuscript. Dirk Schindler developed the research idea, carried out data analysis and wrote the manuscript. Alexander Buchholz processed and mapped storm damage and commented on the manuscript. Axel Tim Albrecht provided storm damage data and commented on the manuscript.

**Conflicts of Interest:** The authors declare no conflict of interest.

## Appendix

**Table A1.** List of symbols, abbreviations and acronyms.

Symbols, Acronyms	Description
<i>ACID</i>	Soil acidification
<i>AUC</i>	Area under curve
<i>DAM<sub>emp</sub></i>	Empirical proportions of storm-damaged timber
<i>DAM<sub>emp,30yr</sub></i>	Empirical proportions of storm-damaged timber in the period 1979–2008
<i>DAM<sub>emp,endemic</sub></i>	Empirical proportions of endemically storm-damaged timber
<i>DAM<sub>emp,i</sub></i>	Empirical proportions of storm-damaged timber in $P_i$
<i>DAM<sub>mod</sub></i>	Modeled proportions of storm-damaged timber
<i>DAM<sub>mod,3*</sub></i>	Modeled proportions of storm-damaged timber in $P_3$ with $GS_{Wiebke}$ being included in model building
<i>DAM<sub>mod,30yr</sub></i>	Modeled proportions of storm-damaged timber in the period 1979–2008
<i>DAM<sub>mod,30yr*</sub></i>	Modeled proportions of storm-damaged timber in the period 1979–2008 with $GS_{Wiebke}$ and $GS_{Lothar}$ being included in model building
<i>DAM<sub>mod,5*</sub></i>	Modeled proportions of storm-damaged timber in $P_5$ with $GS_{Lothar}$ being included in model building
<i>DAM<sub>mod,endemic</sub></i>	Modeled proportions of endemically storm-damaged timber
<i>DAM<sub>mod,i</sub></i>	Modeled proportions of storm-damaged timber in $P_i$
<i>DAM<sub>OOB</sub></i>	OOB samples of modeled proportions of storm-damaged timber
<i>DAM<sub>OOB,i</sub></i>	OOB samples of modeled proportions of storm-damaged timber in $P_i$
<i>DAM<sub>OOB,3*</sub></i>	OOB samples of modeled proportions of storm-damaged timber in $P_3$ with $GS_{Wiebke}$ being included in model building
<i>DAM<sub>OOB,30yr</sub></i>	OOB samples of modeled proportions of storm-damaged timber in the period 1979–2008
<i>DAM<sub>mod,30yr*</sub></i>	OOB samples of modeled proportions of storm-damaged timber in the period 1979–2008 with $GS_{Wiebke}$ and $GS_{Lothar}$ being included in model building
<i>DAM<sub>OOB,5*</sub></i>	OOB samples of modeled proportions of storm-damaged timber in $P_5$ with $GS_{Lothar}$ being included in model building
<i>DAM<sub>OOB,endemic</sub></i>	OOB samples of modeled proportions of endemically storm-damaged timber
<i>DEPTH</i>	Soil depth
<i>FOR</i>	Forest type
<i>GEOL</i>	Geology
<i>GRD</i>	Groundwater affected soils
<i>GS<sub>stat</sub></i>	Statistical gust speed for a return period of five years
<i>GS<sub>stat,Dec</sub></i>	Statistical gust speed of December for a return period of five years
<i>GS<sub>stat,Jan</sub></i>	Statistical gust speed of January for a return period of five years

Table A1. Cont.

Symbols, Acronyms	Description
$GS_{Lothar}$	Gust speed of 26 December 1999
$GS_{Wiebke}$	Gust speed of 1 March 1990
MOIST	Soil moisture regime
MSE	Mean squared error
$PC_{emp,endemic}$	Empirical probability of endemic storm damage events
$PC_{emp,j}$	Empirical classified storm damage probability: ( $j = 1, \dots, 7$ )
$PC_{mod}$	Modeled storm damage probability in percentages
$PC_{mod,j}$	Modeled classified storm damage probability: ( $j = 1, \dots, 7$ )
$PC_{OOB,j}$	OOB samples of modeled classified storm damage probability: ( $j = 1, \dots, 7$ )
$PC_{OOB,mean}$	OOB samples of averaged modeled classified storm damage probability
PI	Predictor Importance
$R^2$	Coefficient of determination
$RC_{emp,endemic}$	Empirical endemic storm damage risk
$RC_{mod,endemic}$	Modeled endemic storm damage risk
$RC_{OOB,endemic}$	OOB samples of modeled endemic storm damage risk
SL	Slope
SOIL	Soil type
SUB	Soil substrate
Abbreviations	Description
OOB	Out-of-bag
$P_{30yr}$	Period from 1979–2008
$P_i$	Five-year period $i$ : 1979–1983 ( $P_1$ ), 1984–1988 ( $P_2$ ), $\dots$ , 2004–2008 ( $P_6$ )
RF	Random forests
ROC	Receiver operating curve

## References

- Franklin, J.F.; Spies, T.A.; van Pelt, R.; Carey, A.B.; Thornburgh, D.A.; Berg, D.R.; Lindenmayer, D.B.; Harmon, M.E.; Keeton, W.S.; Shaw, D.C.; *et al.* Disturbances and structural development of natural forest ecosystems with silvicultural implications, using Douglas-Fir forests as an example. *For. Ecol. Manag.* **2002**, *155*, 399–423. [[CrossRef](#)]
- Stueve, K.M.; Perry, C.H.; Nelson, M.D.; Healey, S.P.; Hill, A.D.; Moisen, G.G.; Cohen, W.B.; Gormanson, D.-D.; Huang, C. Ecological importance of intermediate windstorms rivals large, infrequent disturbances in the northern Great Lakes. *Ecosphere* **2011**, *2*, 2. [[CrossRef](#)]
- Albrecht, A.T.; Fortin, M.; Kohnle, U.; Ningre, F. Coupling a tree growth model with storm damage modeling—Conceptual approach and results of scenario simulations. *Environ. Model. Softw.* **2015**, *69*, 63–76. [[CrossRef](#)]
- Schelhaas, M.-J.; Nabuurs, G.-J.; Schuck, A. Natural disturbances in the European forests in the 19th and 20th centuries. *Glob. Chang. Biol.* **2003**, *9*, 1620–1633. [[CrossRef](#)]
- Gardiner, B.; Blennow, K.; Carbus, J.-M.; Fleischer, P.; Ingemarson, F.; Landmann, G.; Lindner, M.; Marzano, M.; Nicoll, B.; Orazio, C.; *et al.* *Destructive Storms in European Forests: Past and Forthcoming Impacts*; Final Report to European Commission—DG Environment; European Forest Institute: Joensuu, Finland, 2010; p. 138.
- Schüepf, M.; Schiesser, H.H.; Huntrieser, H.; Scherrer, H.U.; Schmidtke, H. The winterstorm “Vivian” of 27 February 1990: About the meteorological development, wind forces and damage situation in the forests of Switzerland. *Theor. Appl. Climatol.* **1994**, *49*, 183–200. [[CrossRef](#)]
- Mayer, H.; Schindler, D. Forstmeteorologische Grundlagen zur Auslösung von Sturmschäden im Wald im Zusammenhang mit dem Orkan “Lothar”. *Allg For. Jgdztg* **2002**, *173*, 200–208. (In German)
- Fink, A.H.; Brücher, T.; Ermert, V.; Krüger, A.; Pinto, J.G. The European storm Kyrill 2007: Synoptic evolution, meteorological impacts and some considerations with respect to climate change. *Nat. Hazards Earth Syst. Sci.* **2009**, *9*, 405–423. [[CrossRef](#)]

9. Kohnle, U.; Gauckler, S.; Risse, F.-J.; Stahl, S. Orkan Lothar im Spiegel von Betriebsinventur und Einschlagsbuchführung: Auswirkungen auf einen Forstbezirk im Randbereich des Sturms. *Allg. Fors. Wald* **2003**, *58*, 1203–1207. (In German)
10. WSL (Eidg. Forschungsanstalt für Wald, Schnee und Landschaft), BUWAL (Bundesamt für Umwelt, Wald und Landschaft). Lothar. Der Orkan 1999. Ereignisanalyse. (eds. WSL, Birmensdorf; BUWAL, Bern), 2001. (In German)
11. Hartebrodt, C. The impact of storm damage on small-scale forest enterprises in the southwest of Germany. *Small Scale For. Econ. Manag. Policy* **2004**, *3*, 203–222.
12. Pasztor, F.; Matulla, C.; Zuvella-Aloise, M.; Rammer, W.; Lexer, M.J. Developing predictive models of wind damage in Austrian forests. *Ann. For. Sci.* **2015**, *72*, 289–301. [[CrossRef](#)]
13. Klopčič, M.; Poljanec, A.; Gartner, A.; Boncina, A. Factors related to natural disturbances in mountain Norway spruce (*Picea abies*) forests in the Julian Alps. *Ecoscience* **2009**, *16*, 48–57. [[CrossRef](#)]
14. Nagel, T.A.; Diaci, J. Intermediate wind disturbance in an old-growth beech-fir forest in southeastern Slovenia. *Can. J. For. Res.* **2006**, *36*, 629–638. [[CrossRef](#)]
15. Schindler, D.; Bauhus, J.; Mayer, H. Wind effects on trees. *Eur. J. For. Res.* **2012**, *131*, 159–163. [[CrossRef](#)]
16. Mayer, H. Wind-induced tree sway. *Trees* **1987**, *1*, 95–106. [[CrossRef](#)]
17. Schindler, D.; Grebhan, K.; Albrecht, A.; Schönborn, J. Modelling the wind damage probability in forests in Southwestern Germany for the 1999 winter storm “Lothar”. *Int. J. Biometeorol.* **2009**, *53*, 543–554. [[CrossRef](#)] [[PubMed](#)]
18. Albrecht, A.; Hanewinkel, M.; Bauhus, J.; Kohnle, U. How does silviculture affect storm damage in forests of south-western Germany? Results from empirical modeling based on long-term observations. *Eur. J. For. Res.* **2012**, *131*, 229–247. [[CrossRef](#)]
19. Schindler, D.; Grebhan, K.; Albrecht, A.; Schönborn, J.; Kohnle, U. GIS-based estimation of the winter storm damage probability in forests: a case study from Baden-Wuerttemberg (Southwest Germany). *Int. J. Biometeorol.* **2012**, *56*, 57–69. [[CrossRef](#)] [[PubMed](#)]
20. Albrecht, A.; Kohnle, U.; Hanewinkel, M.; Bauhus, J. Storm damage of Douglas fir unexpectedly high compared to Norway spruce. *Ann. For. Sci.* **2013**, *70*, 195–207. [[CrossRef](#)]
21. Mitchell, S.J.; Lanquaye-Opoku, N.; Modzelewski, H.; Shen, Y.; Stull, R.; Jackson, P.; Murphy, B.; Ruel, J.-C. Comparison of wind speeds obtained using numerical weather models and topographic exposure indices for predicting windthrow in mountainous terrain. *For. Ecol. Manag.* **2008**, *254*, 193–204. [[CrossRef](#)]
22. Mezei, P.; Grodzki, W.; Blaženec, M.; Jakuš, R. Factors influencing the wind-bark beetles’ disturbance system in the course of an *Ips typographus* outbreak in the Tatra Mountains. *For. Ecol. Manag.* **2014**, *312*, 67–77. [[CrossRef](#)]
23. Nilsson, C.; Goyette, S.; Barring, L. Relating forest damage data to the wind field from high-resolution RCM simulations: Case study of Anatol striking Sweden in December 1999. *Glob. Planet. Chang* **2007**, *57*, 161–176. [[CrossRef](#)]
24. Schmidt, M.; Hanewinkel, M.; Kändler, G.; Kublin, E.; Kohnle, U. An inventory-based approach for modeling single-tree storm damage—Experiences with the winter storm of 1999 in southwestern Germany. *Can. J. For. Res.* **2010**, *40*, 1636–1652. [[CrossRef](#)]
25. Keil, M.; Kiefl, R.; Strunz, G. *CORINE Land Cover 2000—Germany*; Final Report; German Aerospace Center, German Remote Sensing Data Center: Wessling, Germany, 2005; p. 72.
26. Jung, C.; Schindler, D. Statistical Modeling of near-surface wind speed: A case study from Baden-Wuerttemberg (Southwest Germany). *Austin J. Earth Sci.* **2015**, *2*, 1–11.
27. Jung, C.; Schindler, D. Modelling monthly near-surface maximum daily gust speed distributions in Southwest Germany. *Int. J. Climatol.* **2016**. accepted.
28. Belsley, D.A.; Kuh, E.; Welsh, R.E. *Regression Diagnostics*; John Wiley & Sons: New York, NY, USA, 2001.
29. Genuer, R.; Poggi, J.-M.; Tuleau-Malot, C. Variable selection using random forests. *Pattern Recogn. Lett.* **2010**, *31*, 2225–2236. [[CrossRef](#)]
30. Breiman, L. Bagging predictors. *Mach. Learn.* **1996**, *26*, 123–140. [[CrossRef](#)]
31. Prasad, A.-M.; Iverson, L.-R.; Liaw, A. Newer classification and regression tree techniques: Bagging and random forests for ecological prediction. *Ecosystems* **2006**, *9*, 181–199. [[CrossRef](#)]
32. De’ath, G.; Fabricius, K.E. Classification and regression trees: a powerful yet simple technique for ecological data analysis. *Ecology* **2000**, *81*, 3178–3192. [[CrossRef](#)]

33. Dietterich, T.G. An experimental comparison of three methods for constructing ensembles of decision trees: Bagging, boosting, and randomization. *Mach. Learn.* **2000**, *40*, 139–158. [[CrossRef](#)]
34. Khoshgoftaar, T.M.; Xiao, Y.; Gao, K. Software quality assessment using a multi-strategy classifier. *Inform. Sci.* **2011**, *41*, 552–568. [[CrossRef](#)]
35. Svetnik, V.; Liaw, A.; Tong, D.; Culberson, J.C.; Sheridan, R.P.; Feuston, B.P. Random Forest: A classification and regression tool for compound classification and QSAR modeling. *J. Chem. Inf. Comput. Sci.* **2003**, *43*, 1947–1958. [[CrossRef](#)] [[PubMed](#)]
36. Zweig, M.H.; Campbell, G. Receiver-Operating Characteristic (ROC) plots: A fundamental evaluation tool in clinical medicine. *Clin. Chem.* **1993**, *39*, 561–577. [[PubMed](#)]
37. Baker, S.G.; Kramer, B.S. Peirce, Youden, and Receiver Operating Characteristic curves. *Am. Stat.* **2007**, *61*, 343–346. [[CrossRef](#)]
38. Breiman, L. Random forests. *Mach. Learn.* **2001**, *45*, 5–32. [[CrossRef](#)]
39. Gislason, P.O.; Benediktsson, J.A.; Sveinsson, J.R. Random forests for land cover classification. *Pattern Recogn. Lett.* **2006**, *27*, 294–300. [[CrossRef](#)]
40. Jiang, P.; Wu, H.; Wang, W.; Ma, W.; Sun, X.; Lu, Z. MiPred: classification of real and pseudo microRNA precursors using random forest prediction model with combined features. *Nucleic Acids Res.* **2007**, *35*, 339–344. [[CrossRef](#)] [[PubMed](#)]
41. Ni, H.; Chen, A.; Chen, N. Some extensions on risk matrix approach. *Saf. Sci.* **2010**, *48*, 1269–1278. [[CrossRef](#)]
42. Schmid-Haas, P.; Bachofen, H. Die Sturmgefährdung von Einzelbäumen und Beständen. *Schweiz. Z. Forstwes.* **1991**, *6*, 477–504. (In German)
43. Aldinger, E.; Seemann, D.; Konnert, V. Wurzeluntersuchungen auf Sturmwurfflächen 1990 in Baden-Württemberg. *Mitt. Ver. For. Standortkunde u. Forstpflanzenzüchtung* **1996**, *38*, 11–24. (In German)
44. Fuhrer, J.; Beniston, M.; Fischlin, A.; Frei, Ch.; Goyette, S.; Jasper, K.; Pfister, Ch. Climate risks and their impact on agriculture and forests in Switzerland. *Clim. Chang.* **2006**, *79*, 79–102. [[CrossRef](#)]
45. Usbeck, T.; Wohlgemuth, T.; Dobbertin, M.; Pfister, C.; Bürgi, A.; Rebetez, M. Increasing storm damage to forests in Switzerland from 1858 to 2007. *Agric. For. Meteorol.* **2010**, *150*, 47–55. [[CrossRef](#)]
46. Mayer, P.; Brang, P.; Dobbertin, M.; Hallenbarter, D.; Renaud, J.-P.; Walthert, L.; Zimmermann, S. Forest storm damage is more frequent on acidic soils. *Annu. For. Sci.* **2005**, *62*, 303–311. [[CrossRef](#)]
47. Valinger, E.; Fridman, J. Factors affecting the probability of windthrow at stand level as a result of Gudrun winter storm in southern Sweden. *For. Ecol. Manag.* **2011**, *262*, 398–403. [[CrossRef](#)]
48. Hanewinkel, M.; Albrecht, A.; Schmidt, M. Influence of Stand Characteristics and Landscape Structure on Wind Damage. In *What Science Can Tell Us. Living with Storm Damage to Forests*; Gardiner, B., Schuck, A., Schelhaas, M.-J., Orazio, C., Blennow, K., Nicoll, B., Eds.; European Forest Institute: Joensuu, Finland, 2013; pp. 39–45.
49. Klaus, M.; Holsten, A.; Hostert, P.; Kropp, J. Integrated methodology to assess windthrow impacts on forest stands under climate change. *For. Ecol. Manag.* **2011**, *261*, 1799–1810. [[CrossRef](#)]
50. De Langre, E. Effects of Wind on Plants. *Annu. Rev. Fluid Mech.* **2008**, *40*, 141–168. [[CrossRef](#)]
51. Nicoll, B.; Ray, D. Adaptive growth of tree root systems in response to wind action and site conditions. *Tree Physiol.* **1996**, *16*, 891–898. [[CrossRef](#)] [[PubMed](#)]
52. Wilson, J. Vulnerability to wind damage in managed landscapes of the coastal Pacific Northwest. *For. Ecol. Manag.* **2004**, *191*, 341–351. [[CrossRef](#)]
53. Nicoll, B.; Gardiner, B.; Peace, A.J. Improvements in anchorage provided by the acclimation of forest trees to wind stress. *Forestry* **2008**, *81*, 389–398. [[CrossRef](#)]
54. Mitchell, S.J. Wind as a natural disturbance agent in forests: a synthesis. *Forestry* **2013**, *86*, 147–157. [[CrossRef](#)]
55. Heneka, P.; Hofherr, T.; Ruck, B.; Kottmeier, C. Winter storm risk of residential structures—Model development and application to the German state of Baden-Württemberg. *Nat. Hazards Earth Syst. Sci.* **2006**, *6*, 721–733. [[CrossRef](#)]
56. Schütz, J.-P.; Götz, M.; Schmid, W.; Mandallaz, D. Vulnerability of spruce (*Picea abies*) and beech (*Fagus sylvatica*) forest stands to storms and consequences for silviculture. *Eur. J. For. Res.* **2006**, *125*, 291–302. [[CrossRef](#)]
57. Hanewinkel, M.; Breidenbach, J.; Neef, T.; Kublin, E. 77 years of natural disturbances in a mountain forest area—The influence of storm, snow and insect damage analysed with a long-term time series. *Can. J. For. Res.* **2008**, *38*, 2249–2261. [[CrossRef](#)]

58. Hagen, M.; Bartenschlager, B.; Finke, U. Motion characteristics of thunderstorms in southern Germany. *Meteorol. Appl.* **1999**, *6*, 227–239. [[CrossRef](#)]
59. Kunz, M. The skill of convective parameters and indices to predict isolated and severe thunderstorms. *Nat. Hazards Earth Syst. Sci.* **2007**, *7*, 327–342. [[CrossRef](#)]
60. Kunz, M.; Sander, J.; Kottmeier, C.-H. Recent trends of thunderstorm and hailstorm frequency and their relation to atmospheric characteristics in southwest Germany. *Int. J. Climatol.* **2009**, *29*, 2283–2297. [[CrossRef](#)]



© 2016 by the authors; licensee MDPI, Basel, Switzerland. This article is an open access article distributed under the terms and conditions of the Creative Commons by Attribution (CC-BY) license (<http://creativecommons.org/licenses/by/4.0/>).